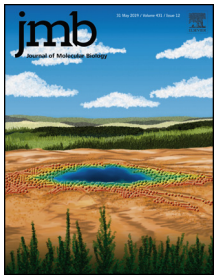

An Interspecies Analysis Reveals Molecular Construction Principles of Interleukin 27

Stephanie I. Müller[1,†], **Isabel Aschenbrenner**[1,†], **Martin Zacharias**[2] and **Matthias J. Feige**[1,]

*1 - **Center for Integrated Protein Science at the Department of Chemistry and Institute for Advanced Study,** Technical University of Munich, 85748 Garching, Germany*
*2 - **Center for Integrated Protein Science at the Physics Department,** Technical University of Munich, 85748 Garching, Germany*

***Correspondence to Martin Zacharias and Matthias J. Feige:** Technical University of Munich, Department of Physics, James-Franck-Str. 1, 85748 Garching, Germany. Technical University of Munich, Department of Chemistry, Lichtenbergstr. 4, 85748 Garching, Germany. martin.zacharias@mytum.de, matthias.feige@tum.de*
https://doi.org/10.1016/j.jmb.2019.04.032
Edited by Amy Keating

Abstract

Interleukin 27 (IL-27) is a cytokine that regulates inflammatory responses. It is composed of an α subunit (IL-27α) and a β subunit (EBI3), which together form heterodimeric IL-27. Despite this general principle, IL-27 from different species shows distinct characteristics: Human IL-27α is not secreted autonomously while EBI3 is. In mice, the subunits show a reciprocal behavior. The molecular basis and the evolutionary conservation of these differences have remained unclear. They are biologically important, however, since secreted IL-27 subunits can act as cytokines on their own.

Here, we show that formation of a single disulfide bond is an evolutionary conserved trait, which determines secretion-competency of IL-27α. Furthermore, combining cell-biological with computational approaches, we provide detailed structural insights into IL-27 heterodimerization and find that it relies on a conserved interface. Lastly, our study reveals a hitherto unknown construction principle of IL-27: one secretion-competent subunit generally pairs with one that depends on the other to induce its secretion.

Taken together, these findings significantly extend our understanding of IL-27 biogenesis as a key cytokine and highlight how protein assembly can influence immunoregulation.

Introduction

Secreted proteins like cytokines, extracellular enzymes or antibodies are produced in the endoplasmic reticulum (ER) and released by cells to interact with their environment. In multicellular organisms, most physiological functions essentially depend on secreted proteins. Interleukins (ILs), as a prime example, mediate immune cell communication. They maintain organism homeostasis by activating or suppressing defense mechanisms. It is thus of utmost importance that secreted ILs possess their correct structure, which defines their biological activity. A dedicated quality control (QC) system in the ER, composed of chaperones and folding enzymes [1,2], ensures that ILs and other secretory proteins fold and assemble correctly before being released into the extracellular space.

For interleukin 27 (IL-27), a member of the heterodimeric IL-12 cytokine family [3,4], cellular QC is not only a means to prevent secretion of aberrant proteins, but also a way to modulate immune reactions: IL-27 consists of the α subunit IL-27α and the β subunit Epstein–Barr virus induced gene 3 (EBI3) [5]. IL-27 is secreted by antigen-presenting cells and signals *via* a heterodimeric receptor composed of IL-27Rα and gp130 to regulate immune functions, mainly by controlling T cell differentiation [4–9]. In mice, IL-27α is stabilized by a single disulfide bond and therefore can pass ERQC and be secreted from cells without its partner subunit EBI3 to act within the murine cytokine repertoire [5,10–13]. In humans, however, IL-27α is incompletely folded in isolation and depends on EBI3 to leave the cell [5,13]. Interestingly, EBI3 behaves reciprocally to IL-27α in these two species: human

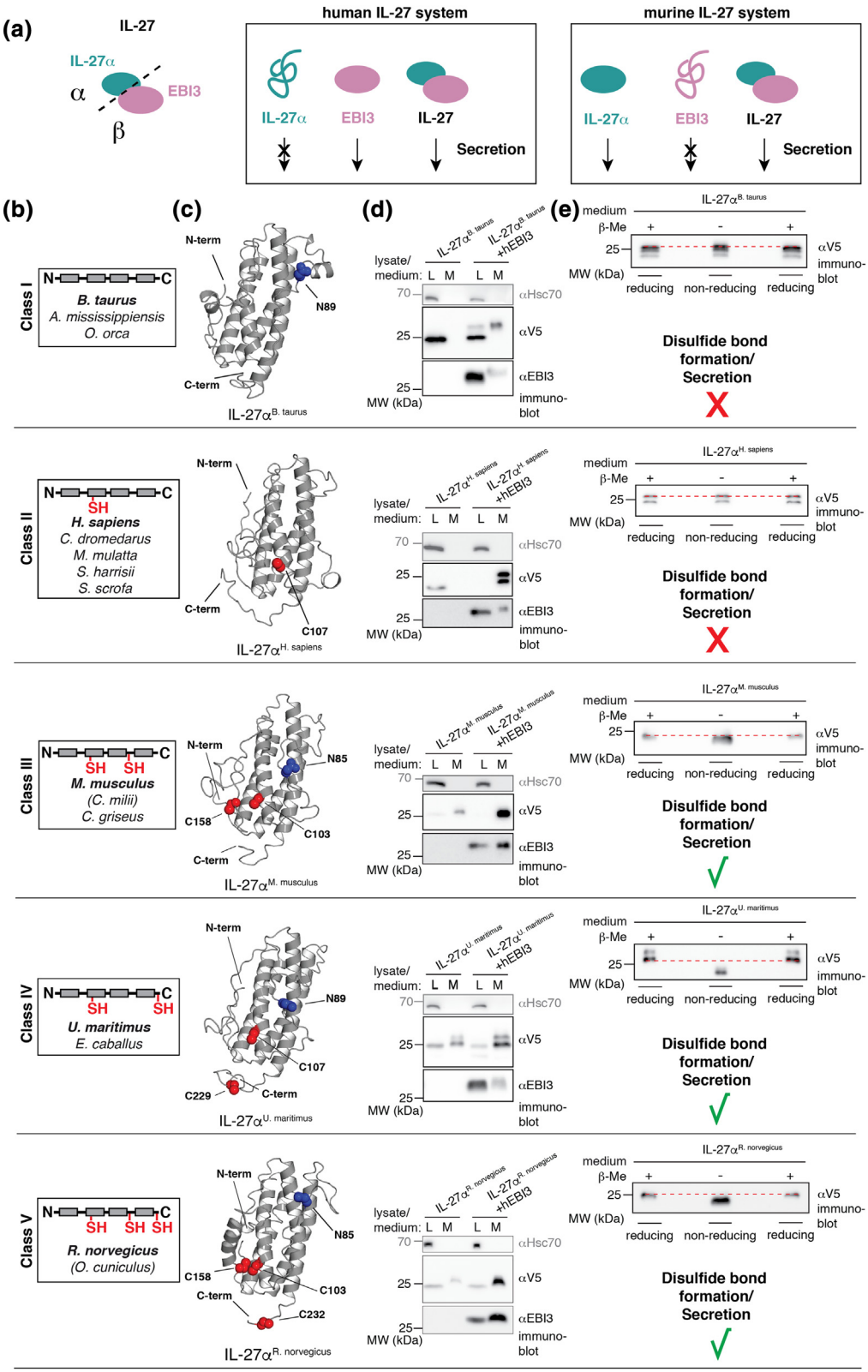

Fig. 1 (*legend on next page*)

EBI3 can be secreted in absence of human IL-27α [5] and has been proposed to be an immunomodulator of maternal tolerance during pregnancy [14]. Murine EBI3, in contrast, is retained in cells and cannot be secreted without its α subunit [5,15]. The molecular mechanisms underlying EBI3 retention *versus* secretion remain unclear. Furthermore, although immunological functions of IL-27 have been well characterized [8,9], its structure remains unresolved. While IL-27α is predicted to have the typical 4-helix bundle structure of type I cytokines [16], EBI3 is homologous to soluble members of the class I cytokine receptor family like IL-6Rα, consisting of two Fibronectin III domains connected by a hinge region [17].

To provide insights into general construction principles of the key cytokine IL-27, further define its structural setup and immunoregulatory capabilities, we pursued an approach combining evolutionary analyses with structural investigations. We define basic criteria of IL-27α and EBI3 secretion and show how the IL-27 system has evolved to maintain immune balance in various organisms.

Results

Disulfide bond formation is an evolutionary conserved determinant for IL-27α secretion

In all species examined, IL-27 is a heterodimeric cytokine composed of IL-27α and EBI3 (Fig. 1a). Its assembly control, however, varies in different organisms: Human IL-27α (hIL-27α) is retained in the cell and can only be secreted upon co-expression of its β subunit EBI3 [5]. Murine IL-27α (mIL-27α), in contrast, is secretion-competent on its own and acts as a cytokine [5,10–12] (Fig. 1a). Very recently, it has been shown that the folding- and secretion-competency of human and murine IL-27α can be changed by introducing or eliminating a single disulfide-bond forming Cys residue, respectively [13]. In order to reveal if disulfide bond formation is a more general, evolutionary conserved trait that defines autonomous IL-27α secretion, we performed a multiple sequence alignment of IL-27α from 15 different species, laying emphasis on the number and location of Cys in the sequences (Supplementary Fig. S1a). This alignment allowed us to group IL-27α into five different classes. These either contain no Cys (class I), a single Cys (class II), two Cys with the second Cys being located centrally (class III) or towards the C-terminus of the protein (class IV), or three Cys (class V) (Fig. 1b and Supplementary Fig. S1a). To structurally understand how the Cys residues are arranged within the proteins, we generated homology models for the various α subunits (Fig. 1c and Supplementary Fig. S1b). The modeled structures illustrate that, whenever present, the first Cys is always located in the second α-helix of IL-27α. The second Cys is located either in a characteristic poly-Glu loop of IL-27α [18] (class III and V) or towards the C-terminus of the protein (class IV), where also the third Cys in class V is located (Fig. 1b and c).

Based on this *in silico* analysis, we proceeded to test two hypotheses concerning IL-27α experimentally. First, that predicted proximity of two Cys in the modeled structure is sufficient for disulfide bond formation to occur. And second, that disulfide bond formation correlates with autonomous secretion of IL-27α. Towards this end, we analyzed the secretion behavior and disulfide bond formation of representatives from each class. In complete agreement with our hypotheses, we found that whenever none or a single Cys was present, IL-27α was dependent on assembly with EBI3 for secretion (classes I and II, Fig. 1b and d and Supplementary Fig. S1b and c). In agreement with this data, IL-27α of classes I and II did not form a disulfide bond (Fig. 1e and Supplementary Fig. S1d). The presence of two or more Cys, however, always

Fig. 1. Folding- and secretion-competency of IL-27α depend on disulfide bond formation. (a) Schematic of the heterodimeric IL-27, consisting of the non-covalently linked subunits IL-27α and EBI3. In humans (left box), IL-27α is retained in cells in isolation and depends on co-expression of EBI3, whereas in mice (right box), IL-27α is secretion-competent and is needed to induce EBI3 secretion. (b) Classification of IL-27α was performed according to the number and location of Cys residues. Species belonging to each class are listed – with the representative species selected for experiments in bold. The location of Cys (red) in helix 2 (box, gray), loop 3 (line, black) and/or the C-terminus (C) are depicted within a schematic structure of IL-27α. Parenthesized species share the same number of Cys but slightly differ in Cys location compared to the class consensus. (c) Homology models of IL-27α subunits from representative species of classes I-V. Within the 4-helix bundle structure, Cys residues (red) and predicted *N*-glycosylation sites (blue) are shown in a CPK representation. (d) Secretion-competency of IL-27α varies between classes. IL-27α of class I (no Cys) or class II (single Cys) is retained in cells in isolation (L), whereas co-expression with human EBI3 (hEBI3) induces its secretion (M). With two or three Cys (classes III, IV and V), IL-27α is secretion-competent even in absence of the β subunit. 2% L/M were applied to the gel and blotted with the indicated antibodies. Hsc70 served as a loading control. (e) Disulfide bond formation as a prerequisite for folding- and secretion-competency of IL-27α. Secretion-competent IL-27α (classes III-V) forms a disulfide bond. Secreted α subunits were analyzed by non-reducing SDS-PAGE and blotted with anti-V5 antibody. 1–2% medium (M) were applied to the gel and blotted with the indicated antibodies. Where indicated (+), samples were treated with β-mercaptoethanol (β-Me) to reduce disulfide bonds. To highlight mobility differences, dashed lines are shown. *N*-glycosylated IL-27α from *B. taurus*, *M. musculus* and *R. norvegicus* were deglycosylated with PNGase F prior to SDS-PAGE analysis. (d, e) L, lysate. M, medium. MW, molecular weight.

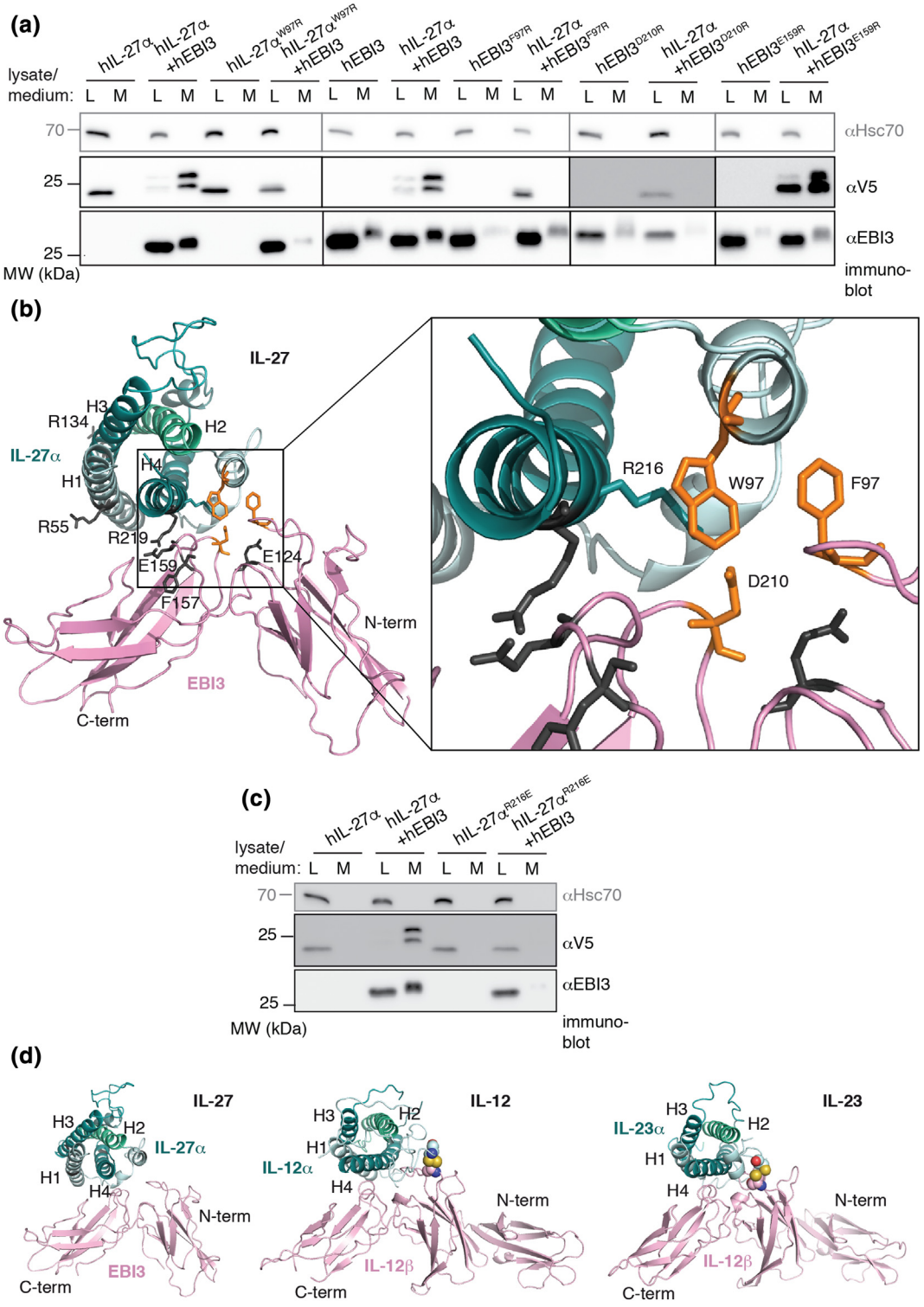

Fig. 2. A structural analysis of IL-27 heterodimerization. (a) hIL-27α^{W97R}, hEBI3^{F97R} and hEBI3^{D210R} but not hEBI3^{E159R} disrupt subunit interactions in IL-27. EBI3^{D210R} contained a C-terminal FLAG-tag. (b) Molecular docking of human IL-27 shows hIL-27α^{W97}, hEBI3^{F97} and hEBI3^{D210} to be located within the interface of the human α and β subunit. Helices 1–4 (H1–4) in IL-27α are indicated. (c) The hIL-27α^{R216E} mutation disrupts IL-27 formation. (d) Comparison of docked IL-27 with IL-12 and IL-23 crystal structures. Disulfide bonds in IL-12 and IL-23 are shown in a CPK representation. Helices 1–4 (H1–4) in the α subunits are indicated. (a, c) L, lysate. M, medium. MW, molecular weight. 2% L/M were applied to the gel and blotted with the indicated antibodies. Hsc70 served as a loading control.

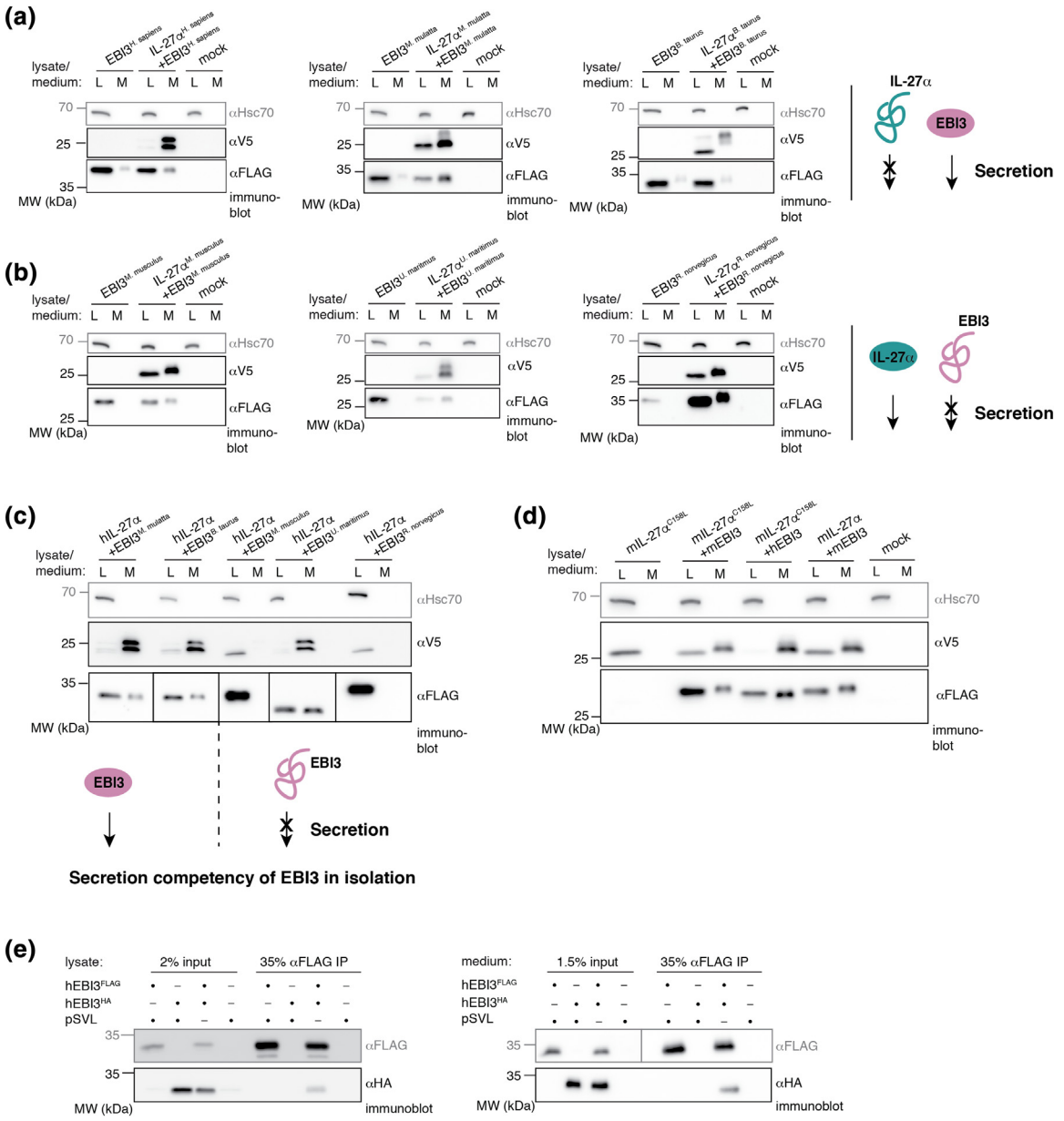

Fig. 3. An evolutionary conserved molecular construction principle of IL-27. (a,b) In all species tested, secretion-competent EBI3 subunits pair with secretion-incompetent IL-27α subunits to form IL-27 and *vice versa*. (a) EBI3 is secretion-competent (M) in isolation whenever its corresponding IL-27α is secretion-incompetent alone. (b) EBI3 from species with secretion-competent IL-27α is secretion-incompetent and thus retained in cells in isolation (L). Darker exposures are shown for EBI3 in Supplementary Fig. S3. (c) Secretion-incompetent hIL-27α was co-expressed with EBI3 from different species, being itself either secretion-competent or -incompetent as indicated. Secretion-incompetent EBI3 proteins were not able to induce hIL-27α secretion except for polar bear EBI3. (d) The secretion-incompetent mIL-27α^{C158L} mutant and mEBI3 mutually induce their secretion. (e) EBI3 forms homodimers. 35% lysate or medium of cells transfected with FLAG-tagged EBI3/mock and/or HA-tagged EBI3 was immunoprecipitated with anti-FLAG antibody, applied together with input samples to the gel and immunoblotted with the indicated antibodies (MW, molecular weight). (a-d) L, lysate. M, medium. MW, molecular weight. 2% L/M were applied to the gel and blotted with the indicated antibodies. Hsc70 served as a loading control.

rendered IL-27α secretion-competent in isolation (classes III, IV and V in Fig. 1b and d). Autonomous secretion of IL-27α was always concurrent with disulfide bond formation (Fig. 1e). In agreement with the structural models, a larger number of residues between Cys connected by an intramolecular disulfide bond resulted in a larger shift of IL-27α under non-reducing conditions on SDS-PAGE gels (*e.g.* mouse *versus* polar bear IL-27α in Fig. 1e). Furthermore, whenever *N*-linked glycosylation sites were predicted

(Fig. 1c and Supplementary Fig. S1a and b), modification of these sites upon secretion could be detected (Fig. 1d and Supplementary Fig. S1c and e). Remarkably, human EBI3 (hEBI3) was able to induce or increase secretion of IL-27α from all species tested (Fig. 1d and Supplementary Fig. S1c). Taken together, our data show that disulfide bond formation is an evolutionary conserved determinant for autonomous secretion and thus potential biological functions of IL-27α. Furthermore, our findings point towards a conserved mode of IL-27 heterodimerization that we next investigated further.

A structural analysis of the IL-27 interface reveals evolutionary conservation

Despite its important immunological functions, no experimentally determined structure is available for IL-27 yet. Thus, to provide further structural insights into IL-27 heterodimerization, we decided to use a mutational approach combined with docking and molecular dynamics (MD) simulations. A broad set of mutations was selected based on i) a previous structural analysis of IL-27 heterodimerization [16], and ii) the homology of IL-27 to CNTF, IL-12 and IL-23 [16,19–22]. This approach led to nine possible interface residues (Fig. 2a and b and Supplementary Fig. S2a), which we tested experimentally by single point mutations. To investigate the effect of the different mutations, we analyzed hEBI3-induced secretion of hIL-27α. Secretion of hIL-27α can be assessed *via O*-glycosylation, which occurs during Golgi passage: while hIL-27α populates a single species only detectable in the lysate (L, Fig. 2a), co-expression of hEBI3 induces secretion into the medium concomitant with the formation of different *O*-glycosylated species (M, Fig. 2a) [13]. Using this assay, we found that in agreement with previous data [16], hIL27a^{W97R}, hEBI3^{F97R} and hEBI3^{D210R} disrupted hIL-27α secretion (Fig. 2a). The hEBI3^{E159R} mutant, in contrast to what has been reported previously [16], did not inhibit hIL-27α secretion in our experiments (Fig. 2a). This is in agreement with studies on mouse EBI3 [23] and may be due to the different assays used: induction of hIL-27α secretion by EBI3 would also report on weak interactions, as opposed to co-immunoprecipitations [16]. All other five residues tested did not inhibit EBI3-induced secretion of hIL-27α (Supplementary Fig. S2b-d). Together, this provided us with a comprehensive set of disruptive and non-disruptive single point mutants, which we used to guide a docking approach combined with MD refinement simulations (Fig. 2b). In the obtained model, Trp97 of hIL-27α is located at the center of the interface and binds at the hinge region between the two domains of hEBI3. It contacts Phe97 and, in addition, several other residues in hEBI3 such as Leu96, Thr209 and Asp210. The model predicts a salt bridge contact between Arg216 in hIL-27α and Asp210 in hEBI3 as well as a stacking contact between Phe94 (hIL-27α) and Phe97 (hEBI3) that further stabilizes binding. In order to test our model experimentally, we substituted Arg216 in hIL-27α with a negatively charged Glu residue, which would interrupt the predicted interaction between hIL-27α Arg216 and hEBI3 Asp210 (Fig. 2b). In complete agreement with our docking, the mutant hIL-27α^{R216E} disrupted IL-27 formation (Fig. 2c). The model was also compatible with all residues found to be of lesser or no importance for binding on both partners (Supplementary Fig. S2a-d) since these residues are not at the interface, with the exception of Arg219 in hIL-27α. However, the guanidinium group of Arg219 does not form any specific contact, *e.g.* a salt bridge with the hEBI3 partner, compatible with the finding that substitution of this residue did not interfere with complex formation (Supplementary Fig. S2c, right panel). Importantly, all the IL-27α residues that form the predicted interface (defined as residues in contact with residues of the hEBI3 partner, *i.e.* a side chain atom-atom distance of <5 Å) are highly conserved among the IL-27α molecules from different species (Supplementary Fig. S2e). This is consistent with our finding that human EBI3 could induce secretion of IL-27α from all tested species (Fig. 1d). Interestingly, despite this fact, some differences appeared to exist in the molecular details of interactions: co-expression of hEBI3^{F97R} could not induce secretion of IL-27α from Tasmanian devil and monkey, like observed for human IL-27α (Fig. 2a and Supplementary Fig. S2f). IL-27α from cow and pig, however, were able to leave the cell in the presence of this mutant (Supplementary Fig. S2f). A comparison of IL-27α residues from these species, predicted to be located at the interface with hEBI3, did not indicate any difference (Supplementary Fig. S2e). Hence, the structural model suggests that the origin of the different behavior of IL-27α from Tasmanian devil and monkey *versus* cow and pig is not associated with residue differences at the subunit interface. It might thus be possible that hEBI3^{F97R} has generally lower affinity to (any) IL-27α and this weak subunit association is sufficient for IL-27α from pig and cow to fold correctly and assemble, whereas it is insufficient in case of IL-27α from Tasmanian devil and monkey.

Similar to the known structures of IL-12 [19] and IL-23 [20], helix 4 (H4) of hIL-27α contributed most to the interface with hEBI3 (Fig. 2d). Interestingly, despite this overall similarity, the arrangement of the hIL-27α subunit relative to the β subunit was slightly rotated and translated in the IL-27 model – which positions the residues found critical for IL-27 formation at the interface – compared to the corresponding placement in the IL-12 and IL-23 complexes (Fig. 2d). A global arrangement like in IL-12 and IL-23 would shift the critical Trp97 in IL-27α away from the interface. Note, that both in the IL-12 and IL-23 complex the arrangement of α and

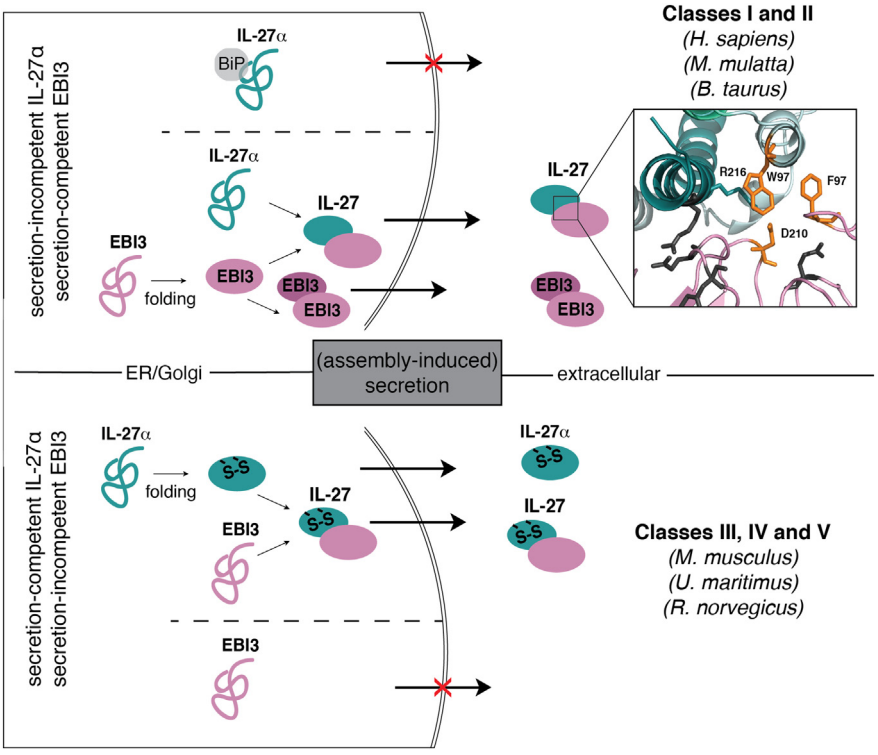

Fig. 4. A model for IL-27 biogenesis. Secretion-incompetent IL-27α (classes I and II) pairs with secretion-competent EBI3 and *vice versa* (classes III, IV and V). Species from which IL-27 was investigated in this study are shown in brackets. Disulfide bond formation (S-S) determines folding and secretion-competency of IL-27α subunits. IL-27α is retained in the cell by BiP binding if no disulfide bond is present [13]. EBI3 can form homodimers (shown for human EBI3 in this study). The inset highlights the heterodimerization interface of human IL-27 as defined in this study.

β partners is stabilized by an intermolecular disulfide bond (Fig. 2d) that is absent in IL-27 and may contribute to the slightly shifted arrangement. Taken together, our approach provides an improved structural model for IL-27 that is compatible with our comprehensive mutational analysis and reveals molecular details of αβ heterodimerization modes within the IL-12 family.

Reciprocally induced secretion of its constituent subunits is an evolutionary conserved trait of IL-27

Reminiscent of the IL-27α subunit, the IL-27β subunit EBI3 shows a different secretion behavior depending on the species. In humans, EBI3 can be secreted without co-expressing its corresponding IL-27α subunit, albeit weakly ([24] and Fig. 3a). In contrast, in mice, IL-27α is needed to induce EBI3 secretion ([5,15] and Fig. 3b). Interestingly, in both species, one secretion-competent subunit thus pairs with one secretion-incompetent subunit to form IL-27, only differing in the allocation of these traits to α or β subunit (depicted by the scheme in Fig. 3a and b on the right). Intrigued by this observation, we investigated if this construction principle was evolutionary conserved by testing the secretion-competency of the β subunit from species, where the α subunit is either secretion-incompetent (monkey and cow) or secretion-competent (polar bear and rat). Strikingly, EBI3 from monkey and cow were secreted into the medium without co-expression of IL-27α (Fig. 3a and Supplementary Fig. S3). Moreover, EBI3 from polar bear and rat were retained in cells in isolation and only secreted into the medium upon co-expression of their secretion-competent α subunits (Fig. 3b and Supplementary Fig. S3). Our data thus suggest that combination of a secretion-competent with a secretion-incompetent subunit is a common construction principle of IL-27. In the light of this finding, we wondered if only IL-27 subunits that co-evolved with assembly-dependent partner subunits were able to induce their secretion. To test this idea, we co-expressed human IL-27α with EBI3 from five different species and analyzed if the subunits were retained in or secreted by the cells (Fig. 3c). In complete agreement with this idea, hIL-27α was well-secreted upon co-expression of secretion-competent monkey and cow EBI3, but was retained in the cell when co-expressed with secretion-incompetent EBI3 from mouse and rat (Fig. 3c). The only exception from this rule was EBI3 from polar bear, which induced hIL-27α secretion comparable to secretion-competent EBI3 species. This pointed towards the interesting possibility that two secretion-incompetent subunits could in principle pair to become secreted together. To further test this, we examined if mEBI3 could induce secretion of the previously described mutant mIL-27α^{C158L}. This mutant is rendered secretion-incompetent in isolation by replacing Cys158 by Leu, removing its disulfide bond [13]. Indeed, co-expression with mEBI3 led to secretion of both subunits, mEBI3 and mIL-27α^{C158L} (Fig. 3d), constituting another

example of two secretion-incompetent subunits that can become secreted together. This finding furthermore underscores that mIL-27α^{C158L} together with mEBI3 recapitulates the behavior of the human system in regard to IL-27α, which qualifies it as a tool to further analyze the IL-27α and IL-27 biology in mouse models.

Lastly, we were wondering in which assembly state EBI3 would be secreted. This is of relevance, since generally two receptor chains are needed to initiate signaling by IL-12 family members [3]. Co-immunoprecipitation experiments of differentially tagged human EBI3 revealed the formation of homodimers in cells as well as in the medium (Fig. 3e), showing that EBI3 can be secreted as a homodimer. In this context it is noteworthy, that the shared IL-12/IL-23 β subunit (IL-12β) can also be secreted autonomously, including formation of a homodimer, and performs immunoregulatory functions [25,26].

Summary

In conclusion, our study reveals that disulfide bond formation is an evolutionary conserved determinant of IL-27α secretion and its potential role as a cytokine (Fig. 4). Furthermore, by an in-depth mutational and computational analysis, we were able to provide detailed insights into the molecular architecture of the IL-27 interface, which will also help in future engineering approaches. And lastly, our study reveals a hitherto unappreciated but intriguing setup of the IL-27 system, where one secretion-competent subunit pairs with one, that needs to assemble in order to be secreted. Our data show that this is not rooted in the biophysics of IL-27 subunit assembly, since we also could generate pairs of two assembly-incompetent subunits that mutually promoted their secretion. This suggests that the combinatorial principle realized for IL-27 has evolved for a functional benefit rather than due to structural requirements, *e.g.* to maintain a functional and balanced immune system. Using different protein assembly states with distinct functionalities appears to be a common design principle in immune systems to extend the signaling repertoire of cytokines and maintain immune homeostasis [12,13,25,27–29].

Materials and methods

Constructs for mammalian expression

For mammalian expression, all interleukin cDNAs were cloned into the pSVL vector (Amersham BioSciences). Human interleukin cDNAs (hIL-27α and hEBI3) were obtained from OriGene and amino acid sequences correspond to the UniProt accession numbers Q8NEV9 and Q14213, respectively. For a species comparison of IL-27α, sequences corresponding to GenBank identifiers NP_001158125.1 (*Bos taurus*), EHH31550.1 (*Macaca mulatta*), NP_663611.1 (*Mus musculus*), XP_344963.5 (*Rattus norvegicus*), XP_012398754.1 (*Sarcophilus harrisii*) and XP_008683452.1 (*Ursus maritimus*) were synthesized by GeneArt (Thermo Fisher Scientific) with optimized codon-usage for human expression. A $(GS)_4$-linker followed by a V5-tag was introduced at the C-terminus of the different IL-27α constructs. For a species comparison of EBI3, sequences corresponding to GenBank identifiers AAI49503.1 (*Bos taurus*), XP_014977995.1 (*Macaca mulatta*), NP_001102891.1 (*Rattus norvegicus*) and XP_008709480.1 (*Ursus maritimus*) were synthesized by GeneArt with optimized codon-usage for human expression (Thermo Fisher Scientific). Mouse EBI3 cDNA, according to GenBank identifier NM_015766.2 (*Mus musculus*), was obtained from OriGene. Where indicated, EBI3 genes were C-terminally tagged with a $(GS)_4$-linker followed by a FLAG- or an HA-tag. Mutants were generated by site-directed mutagenesis. All constructs were sequenced.

Cell culture and transient transfections

Human embryonic kidney (HEK) 293 T cells were cultured in Dulbecco's modified Eagle's medium (DMEM) containing L-Ala-L-Gln (AQmedia, Sigma-Aldrich) supplemented with 10% (v/v) fetal bovine serum (FBS; Biochrom or Gibco, Thermo Fisher Scientific) at 37 °C and 5% CO_2. The medium was complemented with a 1% (v/v) antibiotic-antimycotic solution (25 µg/ml amphotericin B, 10 mg/ml streptomycin and 10,000 units of penicillin; Sigma-Aldrich) (complete DMEM). Transient transfections were carried out in in either poly D-lysine coated p35 or p60 dishes (BioCoat, Corning) or p60 dishes (Corning BioCoat) using GeneCellin (BioCellChallenge) according to the manufacturer's instructions. Equal amounts of constructs or empty vector were transfected with a total DNA amount of 2 µg (p35) or 4 µg (p60).

Secretion and redox experiments

For secretion and redox-status experiments by immunoblotting, cells were transfected for 8 h, washed twice with phosphate buffered saline (PBS; Sigma-Aldrich) and then supplemented with fresh medium for another 16 h. To analyze secreted proteins, the medium was centrifuged for 5 min, 300 *g*, 4 °C. Subsequently, the supernatant was transferred into a new reaction tube and supplemented with 0.1 volumes of 500 mM Tris/HCl, pH 7.5, 1.5 M NaCl, complemented with 10x Roche complete Protease Inhibitor w/o EDTA (Roche Diagnostics). Prior to lysis, cells were

washed twice in ice-cold PBS. Cell lysis was carried out in RIPA buffer (50 mM Tris/HCl, pH 7.5, 150 mM NaCl, 1.0% Nonidet P40 substitute, 0.5% sodium deoxycholate, 0.1% SDS, 1x Roche complete Protease Inhibitor w/o EDTA; Roche Diagnostics) on ice. Both lysate and medium samples were centrifuged for 15 min, 20,000 g, 4 °C. *N*-glycosylated IL-27α from *B. taurus*, *S. harrissii, M. musculus* and *R. norvegicus* were deglycosylated with PNGase F (SERVA) under non-reducing conditions according to the manufacturer's instructions prior to running redox gels to improve visibility of disulfide-induced down-shifts of proteins on SDS-polyacrylamide gel electrophoresis (PAGE) gels. Endo H (New England Biolabs) deglycosylation experiments were carried out according to the protocol of the manufacturer. Samples were supplemented with 0.2 volumes of 5x Laemmli buffer (0.3125 M Tris/HCl pH 6.8, 10% SDS, 50% glycerol, bromphenol blue) containing either 10% (v/v) β-mercaptoethanol (β-Me) for reducing SDS-PAGE or 100 mM *N*-Ethylmaleimide (NEM) for non-reducing SDS-PAGE.

Immunoprecipitation experiments

For co-immunoprecipitation (co-IP) experiments of FLAG-tagged proteins, cells were washed twice with ice-cold PBS. Cell lysis was carried out in Triton buffer (50 mM Tris/HCl, pH 7.5, 150 mM NaCl, 1 mM EDTA, 1% Triton X-100, 1x Roche complete Protease Inhibitor w/o EDTA; Roche Diagnostics) on ice. Lysates were cleared by centrifugation at 20,000 *g*, 15 min, 4 °C. ANTI-FLAG M2 Affinity Gel (Sigma-Aldrich, A2220) was used for immunoprecipitation according to the manufacturer's protocol using Triton buffer for washes. Proteins were eluted by adding 2x Laemmli buffer (supplemented with 4% (v/v) β-Me) and boiling at 95 °C for 5 min. For immunoprecipitations of secreted proteins, the medium was treated as described for the analysis of secreted protein and subsequently treated like the lysate, using ANTI-FLAG M2 Affinity Gel.

Immunoblotting

For immunoblots, samples were run on 12% SDS-PAGE gels or 8–16% gradient gels (Bio-Rad, for redox experiments of IL-27α *M. musculus* and *R. norvegicus*) and transferred to polyvinylidene difluoride (PVDF) membranes by blotting overnight (o/n) at 30 V and 4 °C. Thereafter, membranes were blocked for at least 3 h with Tris-buffered saline (TBS) containing skim milk powder and Tween-20 (M-TBST; 25 mM Tris/HCl, pH 7.5, 150 mM NaCl, 5% *w/v* skim milk powder, 0.05% v/v Tween-20) or gelatin buffer (0.1% gelatin, 15 mM Tris/HCl, pH 7.5, 130 mM NaCl, 1 mM EDTA, 0.1% Triton X-100, 0.002% NaN_3) for Hsc70 immunoblots. Binding of the primary antibody was carried out o/n at 4 °C with anti-Hsc70 (Santa Cruz, sc-7298, 1:1000) in gelatin buffer, anti-V5 (Abcam, ab27671, 1:1000), anti-FLAG (Sigma-Aldrich, F7425, 1:1000) and anti-HA (BioLegend, 902,302, 1:1000) antibodies in M-TBST. Anti-EBI3 (1:20 in PBS) antiserum has been described previously [14]. Species-specific HRP-conjugated secondary antibodies (Santa Cruz Biotechnology; 1:10,000 in M-TBST) were used. Immunoblots were detected using Amersham ECL prime (GE Healthcare) and a Fusion Pulse 6 imager (Vilber Lourmat).

Sequence analysis, homology modeling and structural analyses

Multiple DNA sequence alignments were performed using Clustal Omega [30] and depicted with BoxShade server (EMBnet). Homology models of isolated IL-27α subunits were generated using iTasser [38]. For generating starting structures for protein–protein docking we followed the homology modeling procedure of Rousseau *et al.* [16]. It is based on a structure-based alignment of IL-27α and hEBI3 sequences to the IL-6 family of cytokines. Structural models of hIL-27α and hEBI3 were generated using the program Modeller [31] and are based on the alignment with known ciliary neurotrophic factor (CNTF) cytokine (pdb: 1cnt) and IL-6 (pdb: 1p9m) structures. For structure modeling the alignments as published by Rousseau *et al.* [16] were used. Generated models were energy minimized (5000 steps) using the Amber18 package [32]) to remove any residual sterical overlap. Docking searches were performed using the protein–protein docking program ATTRACT [33,34]. In ATTRACT, partner proteins are represented by a reduced protein model with four centers per residue [35] to allow rapid energy minimization of docked complexes. The initial search was restricted to starting placements in the vicinity of ~ 20 Å from the Trp97 residue on the hIL-27α side and to ~20 Å from Phe97, Asp210 on the hEBI3 partner protein. Substitution of any of these three residues was found experimentally to disrupt hIL-27α secretion induced by hEBI3. Hence, it is reasonable to assume that these residues are located at the protein–protein interface. Initial docking geometries were energy minimized and favorable docking solutions were screened for geometries with residues hIL-27α Trp97 and hEBI3 Phe97, Asp210 located at the interface and residues substitutions not affecting binding outside of the interface. The most favorable binding geometry was refined at atomic resolution after superimposing the atomistic model structures onto the docked model complex. Refinement was performed by energy minimization (5000 steps) followed by atomistic MD simulation (5 ns using the Amber18 package [32]) and first using an implicit (generalized Born) solvation model [36] for 5 ns at 300 K. A center of mass distance restraint between protein partners was included to avoid dissociation during the refinement step because of possible sterical overlap in the starting structure. For further relaxation of sterical strain the structure was

solvated in explicit TIP3P water [37] and equilibrated for another 10 ns at 300 K at constant pressure (1 bar) after heating up the system over a time frame of 1 ns. The resulting structure fulfilled the experimental restraints such that all residues critical for binding are at the interface and those substitution positions that were found experimentally not to affect binding are all located >6 Å (mostly >10 Å) from the binding interface. An exception is Arg219 in hIL-27α that is located at the rim of the protein–protein interface (Fig. 2b). However, the side chain of Arg219 is not forming specific (*e.g.* salt bridge) contacts to the hEBI3 partner. In the final model hIL-27α Trp97 is in contact with several aromatic and non-polar interface residues of hEBI3 (including hEBI3 Phe97). The Asp210 in hEBI3 forms a salt bridge with Arg216 of hIL-27α. Visualization and structural alignments and further structural analyses were performed using Yasara Structure (www.yasara.org) and PyMOL (PyMOL Molecular Graphics System, Version 2.0 Schrödinger, LLC).

Acknowledgements

We are grateful to Odile Devergne, INSERM/France, for the kind gift of anti-EBI3 antiserum. SIM gratefully acknowledges a PhD scholarship by the German Academic Scholarship Foundation. MJF is a Rudolf Mößbauer Tenure Track Professor and as such gratefully acknowledges funding through the Marie Curie COFUND program and the Technical University of Munich Institute for Advanced Study, funded by the German Excellence Initiative and the European Union Seventh Framework Program under Grant Agreement 291763. MJF gratefully acknowledges funding of our work on interleukins by the Daimler and Benz Stiftung. This work was performed in the framework of the German Research Foundation (DFG) Sonderforschungsbereich 1035, projects B02 and B11.

Author contributions

MJF and SIM conceived the experimental part of the study, MZ conceived the docking part. All experiments were performed by SIM and IA. MZ performed docking simulations. All authors analyzed data and wrote the paper.

Conflict of interest

The authors declare no conflict of interest.

Appendix A. Supplementary data

Supplementary data to this article can be found online at https://doi.org/10.1016/j.jmb.2019.04.032.

Received 25 March 2019;
Received in revised form 18 April 2019;
Accepted 19 April 2019
Available online 26 April 2019

Keywords:
Interleukins;
Protein assembly;
Protein docking;
Protein evolution

†These authors contributed equally to this work.

References

[1] I. Braakman, N.J. Bulleid, Protein folding and modification in the mammalian endoplasmic reticulum, Annu. Rev. Biochem. 80 (2011) 71–99.
[2] M.H. Smith, H.L. Ploegh, J.S. Weissman, Road to ruin: targeting proteins for degradation in the endoplasmic reticulum, Science. 334 (2011) 1086–1090.
[3] D.A. Vignali, V.K. Kuchroo, IL-12 family cytokines: immunological playmakers, Nat. Immunol. 13 (2012) 722–728.
[4] C.A. Hunter, R. Kastelein, Interleukin-27: balancing protective and pathological immunity, Immunity. 37 (2012) 960–969.
[5] S. Pflanz, J.C. Timans, J. Cheung, R. Rosales, H. Kanzler, J. Gilbert, et al., IL-27, a heterodimeric cytokine composed of EBI3 and p28 protein, induces proliferation of naive CD4(+) T cells, Immunity. 16 (2002) 779–790.
[6] S. Pflanz, L. Hibbert, J. Mattson, R. Rosales, E. Vaisberg, J. F. Bazan, et al., WSX-1 and glycoprotein 130 constitute a signal-transducing receptor for IL-27, J. Immunol. 172 (2004) 2225–2231.
[7] G. Trinchieri, S. Pflanz, R.A. Kastelein, The IL-12 family of heterodimeric cytokines: new players in the regulation of T cell responses, Immunity. 19 (2003) 641–644.
[8] S. Aparicio-Siegmund, C. Garbers, The biology of interleukin-27 reveals unique pro- and anti-inflammatory functions in immunity, Cytokine Growth Factor Rev. 26 (2015) 579–586.
[9] H. Yoshida, C.A. Hunter, The immunobiology of interleukin-27, Annu. Rev. Immunol. 33 (2015) 417–443.
[10] S. Crabe, A. Guay-Giroux, A.J. Tormo, D. Duluc, R. Lissilaa, F. Guilhot, et al., The IL-27 p28 subunit binds cytokine-like factor 1 to form a cytokine regulating NK and T cell activities requiring IL-6R for signaling, J. Immunol. 183 (2009) 7692–7702.
[11] J.S. Stumhofer, E.D. Tait, W.J. Quinn III, N. Hosken, B. Spudy, R. Goenka, et al., A role for IL-27p28 as an antagonist of gp130-mediated signaling, Nat. Immunol. 11 (2010) 1119–1126.
[12] C. Garbers, B. Spudy, S. Aparicio-Siegmund, G.H. Waetzig, J. Sommer, C. Holscher, et al., An interleukin-6 receptor-dependent molecular switch mediates signal transduction of the IL-27 cytokine subunit p28 (IL-30) via a gp130 protein receptor homodimer, J. Biol. Chem. 288 (2013) 4346–4354.
[13] S.I. Muller, A. Friedl, I. Aschenbrenner, J. Esser-von Bieren, M. Zacharias, O. Devergne, et al., A folding switch regulates interleukin 27 biogenesis and secretion of its alpha-subunit as a cytokine, Proc. Natl. Acad. Sci. U. S. A. 116 (2019) 1585–1590.
[14] O. Devergne, A. Coulomb-L'Hermine, F. Capel, M. Moussa, F. Capron, Expression of Epstein-Barr virus-induced gene 3, an interleukin-12 p40-related molecule, throughout human

pregnancy: involvement of syncytiotrophoblasts and extravillous trophoblasts, Am. J. Pathol. 159 (2001) 1763–1776.
[15] O. Shimozato, A. Sato, K. Kawamura, M. Chiyo, G. Ma, Q. Li, et al., The secreted form of p28 subunit of interleukin (IL)-27 inhibits biological functions of IL-27 and suppresses anti-allogeneic immune responses, Immunology. 128 (2009) 816–825.
[16] F. Rousseau, L. Basset, J. Froger, N. Dinguirard, S. Chevalier, H. Gascan, IL-27 structural analysis demonstrates similarities with ciliary neurotrophic factor (CNTF) and leads to the identification of antagonistic variants, Proc. Natl. Acad. Sci. U. S. A. 107 (2010) 19420–19425.
[17] M.J. Boulanger, D.C. Chow, E.E. Brevnova, K.C. Garcia, Hexameric structure and assembly of the interleukin-6/IL-6 alpha-receptor/gp130 complex, Science. 300 (2003) 2101–2104.
[18] A.J. Tormo, L.A. Beaupre, G. Elson, S. Crabe, J.F. Gauchat, A polyglutamic acid motif confers IL-27 hydroxyapatite and bone-binding properties, J. Immunol. 190 (2013) 2931–2937.
[19] C. Yoon, S.C. Johnston, J. Tang, M. Stahl, J.F. Tobin, W.S. Somers, Charged residues dominate a unique interlocking topography in the heterodimeric cytokine interleukin-12, EMBO J. 19 (2000) 3530–3541.
[20] P.J. Lupardus, K.C. Garcia, The structure of interleukin-23 reveals the molecular basis of p40 subunit sharing with interleukin-12, J. Mol. Biol. 382 (2008) 931–941.
[21] N.Q. McDonald, N. Panayotatos, W.A. Hendrickson, Crystal structure of dimeric human ciliary neurotrophic factor determined by MAD phasing, EMBO J. 14 (1995) 2689–2699.
[22] F. Rousseau, S. Chevalier, C. Guillet, E. Ravon, C. Diveu, J. Froger, et al., Ciliary neurotrophic factor, cardiotrophin-like cytokine, and neuropoietin share a conserved binding site on the ciliary neurotrophic factor receptor alpha chain, J. Biol. Chem. 283 (2008) 30341–30350.
[23] L.L. Jones, V. Chaturvedi, C. Uyttenhove, J. Van Snick, D.A. Vignali, Distinct subunit pairing criteria within the heterodimeric IL-12 cytokine family, Mol. Immunol. 51 (2012) 234–244.
[24] O. Devergne, M. Birkenbach, E. Kieff, Epstein-Barr virus-induced gene 3 and the p35 subunit of interleukin 12 form a novel heterodimeric hematopoietin, Proc. Natl. Acad. Sci. U. S. A. 94 (1997) 12041–12046.
[25] F.P. Heinzel, A.M. Hujer, F.N. Ahmed, R.M. Rerko, In vivo production and function of IL-12 p40 homodimers, J. Immunol. 158 (1997) 4381–4388.
[26] S.Y. Lee, Y.O. Jung, D.J. Kim, C.M. Kang, Y.M. Moon, Y.J. Heo, et al., IL-12p40 homodimer ameliorates experimental autoimmune arthritis, J. Immunol. 195 (2015) 3001–3010.
[27] D. Chow, X. He, A.L. Snow, S. Rose-John, K.C. Garcia, Structure of an extracellular gp130 cytokine receptor signaling complex, Science. 291 (2001) 2150–2155.
[28] E.H. Duitman, Z. Orinska, E. Bulanova, R. Paus, S. Bulfone-Paus, How a cytokine is chaperoned through the secretory pathway by complexing with its own receptor: lessons from interleukin-15 (IL-15)/IL-15 receptor alpha, Mol. Cell. Biol. 28 (2008) 4851–4861.
[29] G. Espigol-Frigole, E. Planas-Rigol, H. Ohnuki, O. Salvucci, H. Kwak, S. Ravichandran, et al., Identification of IL-23p19 as an endothelial proinflammatory peptide that promotes gp130-STAT3 signaling, Sci. Signal. 9 (2016) ra28.
[30] F. Sievers, A. Wilm, D. Dineen, T.J. Gibson, K. Karplus, W. Li, et al., Fast, scalable generation of high-quality protein multiple sequence alignments using Clustal omega, Mol. Syst. Biol. 7 (2011) 539.
[31] A. Sali, T.L. Blundell, Comparative protein modelling by satisfaction of spatial restraints, J. Mol. Biol. 234 (1993) 779–815.
[32] T.S. Lee, D.S. Cerutti, D. Mermelstein, C. Lin, S. LeGrand, T. J. Giese, et al., GPU-accelerated molecular dynamics and free energy methods in Amber18: performance enhancements and new features, J. Chem. Inf. Model. 58 (2018) 2043–2050.
[33] M. Zacharias, Protein-Protein Docking with a Reduced Protein Model Accounting for Side-Chain Flexibility, Protein Sci. vol. 12 (2003) 1271–1282.
[34] S.J. de Vries, C.E. Schindler, I. Chauvot de Beauchene, M. Zacharias, A web interface for easy flexible protein-protein docking with ATTRACT, Biophys. J. 108 (2015) 462–465.
[35] S. Fiorucci, M. Zacharias, Binding site prediction and improved scoring during flexible protein-protein docking with ATTRACT, Proteins. 78 (2010) 3131–3139.
[36] J. Mongan, C. Simmerling, J.A. McCammon, D.A. Case, A. Onufriev, Generalized born model with a simple, robust molecular volume correction, J. Chem. Theory Comput. 3 (2007) 156–169.
[37] W.L. Jorgensen, C. Jenson, Temperature dependence of TIP3P, SPC, and TIP4P water from NPT Monte Carlo simulations: seeking temperatures of maximum density, J. Comput. Chem. 19 (1998) 1179–1186.
[38] J. Yang, R. Yan, A. Roy, D. Xu, J. Poisson, Y. Zhang, The I-TASSER Suite: Protein structure and function prediction, Nat. Methods 12 (2015) 7–8.